Paper presented at the IET ACDC 2012 conference
in Birmingham, UK, December 4 - 5, 2012

Real-Time Simulation of a Wind Connected HVDC Grid

Pinaki Mitra*, Lidong Zhang¤

**Grid Systems R&D, ABB India, pinaki.mitra@in.abb.com,¤Corporate Research, ABB Sweden, lidong.zhang@se.abb.com*

Keywords: Power-synchronization control, DC grid, wind farm, real-time digital simulator.

Abstract

Real-time simulation of a three-terminal high-voltage direct-current (HVDC) grid connected to a doubly-fed induction generator (DFIG) based wind farm has been presented in this paper. A recently invented control strategy, known as power-synchronization control, is applied for the integration of the wind farm to the HVDC grid. The dynamic performance study of the system under normal wind power fluctuations with wind speed and under some severe fault situations have been studied to demonstrate the effectiveness of the control strategy.

1 Introduction

The rapid increase in electricity consumption all over the world is pushing the high-voltage alternating-current (HVAC) grid to operate very close to its limits. In addition to that, the increased penetration of wind energy is presenting new challenges before the existing HVAC grid. In this new scenario, the idea of high-voltage direct-current (HVDC) grid is emerging to provide a backbone to the existing AC networks and to facilitate the integration of bulk amount of offshore wind power.

Due to the lower losses in DC cables, HVDC transmission has become more popular than HVAC for long distance offshore wind integration. Moreover, HVDC firewalls the offshore wind park from the mainland ac network. The HVDC transmission can be based on either line-commutated converters (LCCs) or voltage-source converters (VSCs). Among them, VSC-HVDC technology is particularly suitable for DC grid formation and integration of offshore wind farms because it does not need any additional reactive-power support and does not depend on external voltage sources for commutation.

Generally speaking, a DC grid can be defined as a VSC based multi-terminal HVDC grid, where several converter terminals are connected in parallel with the DC buses [1]. The advantages of such a DC grid can be summarized as follows: a) reduction in the number of converters compared to several point-to-point HVDC connections [2, 3], b) improved power flow control and energy trading [2], c) reduction in the effect of intermittency for offshore wind connections [3].

In order to validate the newly developed ideas and to verify the control and protection strategies of such a DC grid, ABB has developed a state-of-the-art real-time hardware-in-loop simulation centre. The prime objective of the DC grid simulation centre is to develop a real-time simulation setup for a multi-terminal HVDC system connecting several unsynchronized HVAC grids and offshore wind farms. As a preliminary step towards that goal, a three-terminal HVDC grid is modelled in real-time digital simulator (RTDS) platform, which will serve as a building block for the future research on DC grid. One of the terminals of the modelled DC grid is connected to a doubly-fed induction generator (DFIG) based wind farm. It is worth-mentioning that almost all the basic and some advanced features of ABB's control strategy for the VSC-HVDC stations, which are otherwise carried out in MACH-2 platform for the real-life projects, have been incorporated inside the RTDS based internal controllers.

The successful operation of a VSC-HVDC link depends heavily on the control of grid-connected VSCs. Out of different control strategies; vector-current control is most commonly used by the industries due to its current limiting capability and efficient decoupling of active and reactive powers. However, for a very weak network, the vector-current control finds it difficult to produce expected results [4, 5]. As an alternative, a new approach called power-synchronization control [4] has been proposed recently where, instead of conventional PLL, the synchronization of the VSC with the grid is done through the active power control loop [6]. Due to this feature, the control strategy is capable of connecting to a very weak ac system [7] as well as island system [6] or offshore wind farm. In this paper power-synchronization control has been applied for integrating an offshore wind farm to the three-terminal DC grid.

The rest of the paper is organized as follows: Section 2 describes the test system including the RTDS hardware specifications. The control strategy of the HVDC converter stations as well as of the wind farm converters have been presented in Section 3. It also includes the principle of operation of the power-synchronization control and how it has been utilized for the wind farm integration. Some typical results are shown in Section 4 to demonstrate the performance of the controllers. Finally conclusions and scope of future works have been mentioned in Section 5.

2 Test System

The schematic diagram of the three-terminal test system including the wind farm has been shown in Fig. 1. Among the

three stations, station 1 is connected to a DFIG based wind farm and the other two stations are connected to three-phase ideal voltage sources behind small impedance as shown in Fig. 1. The AC sides of the converters are connected to the point of common coupling (PCC) through a 425kV/400kV transformer with tap changer. The DC side pole-to-ground voltage of the system is kept at 320 kV. At this stage the HVDC converter stations consist of two-level VSC. However, migration to cascaded two-level (CTL) converter models will be carried out in near future. The DFIG converters are also two-level converters connected to a common DC link. The active and reactive power capabilities of all the converter stations are +/-600 MW and +/-250 MVAR respectively.

The entire test system is modelled in three PB5 processor cards in RTDS, each having two PowerPC RISC processors (Freescale MC7448 RISC) operating at a clock frequency of 1.7 GHz. In the test system, all the HVDC converter stations are modelled inside three separate small time-step subnetworks with a time step of 1.5-3 µs. Whereas, for the DFIG based wind farm model, the induction motor and the back-to-back converters stay inside another small time-step subnetwork. All the small time-step VSC subnetworks are interfaced with the large time-step AC systems through interfacing transformers. On the DC side of the HVDC stations, the small time-step VSC subnetworks are connected to each other through travelling wave models of transmission lines. In order to represent a very large capacity wind farm (600 MW) in RTDS, first a 2 MW wind turbine model is developed in small-time-step along with detail converter controls and then a scale-up transformer is used to scale it up to the desired power level.

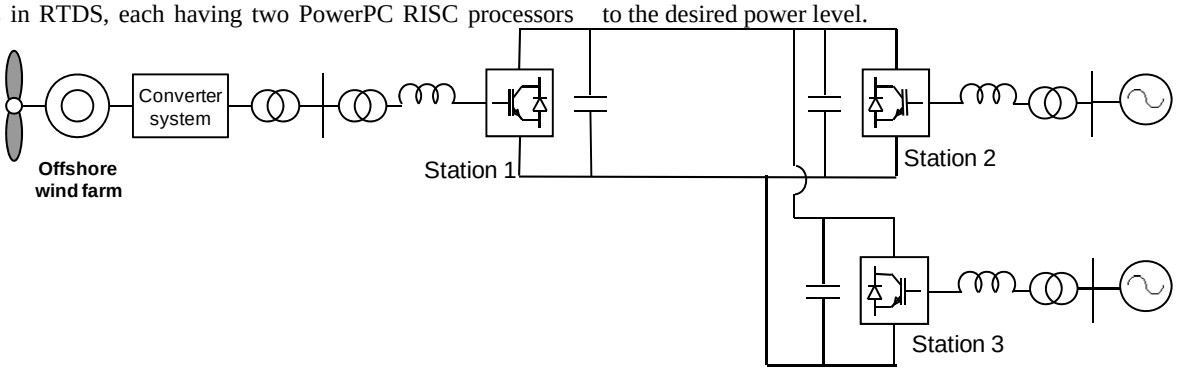

Figure 1: The three-terminal DC grid including wind farm

3 Control Strategy

There are altogether five converters in the system, out of which two are rotor side and grid side converters for the DFIG based wind farm, and the remaining three are HVDC converters. Among the HVDC converter stations, the one which is connecting the offshore wind farm (station 1) employs power-synchronization control and the rest of the stations are based on normal vector-current control. In the following sub-sections, the general control strategy of the HVDC converters are discussed first followed by the power-synchronization control and the control of the wind farm converters.

3.1 Generalized control strategy of HVDC converters

The control strategy of a point-to-point VSC-HVDC connection is shown in Fig. 2. Under normal circumstances, one of the converters controls the DC voltage and the other converter controls the active power. In case of a multi-terminal DC grid, only one station remains in DC voltage control mode and the remaining stations can be in active power control mode. If one of the stations connects to a wind farm as in the test system described here, the station might have to take care of the magnitude and frequency of the ac voltage of the wind farm collection bus. Moreover, it is generally recommended to incorporate additional DC voltage control function in all the power controlling stations, so that in case of faults in the DC voltage controlling station, the DC voltage can be controlled by the other power controlling stations. Apart from the wind farm interconnecting converter, all the other converter stations can be switched between reactive power and AC voltage control mode. For the test system presented in this paper, station 2 is kept in DC voltage control mode and station 3 is kept in active power control mode. Since stations 2 and 3 are connected to strong AC grids, instead of AC voltage control reactive power control mode is activated for the stations.

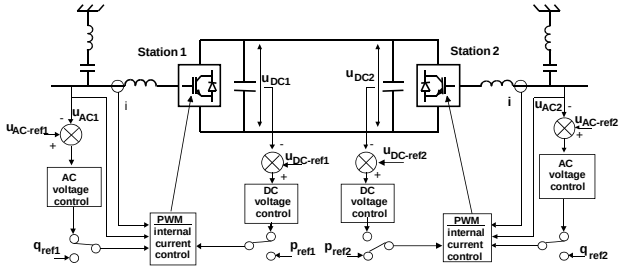

Figure 2: The control strategy of point-to-point HVDC link

3.2 Power-synchronization control

The schematic diagram of power-synchronization control has been presented in Fig. 3. The synchronization with the ac system is done through the power-synchronization loop (PSL) which follows the simple control law as shown in (1)

$$\theta_v = \frac{k_p}{s}(P_{ref} - P) \qquad (1)$$

The other control law, named as alternating-voltage control (AVC), generates the change in VSC reference voltage (ΔV) as in (2)

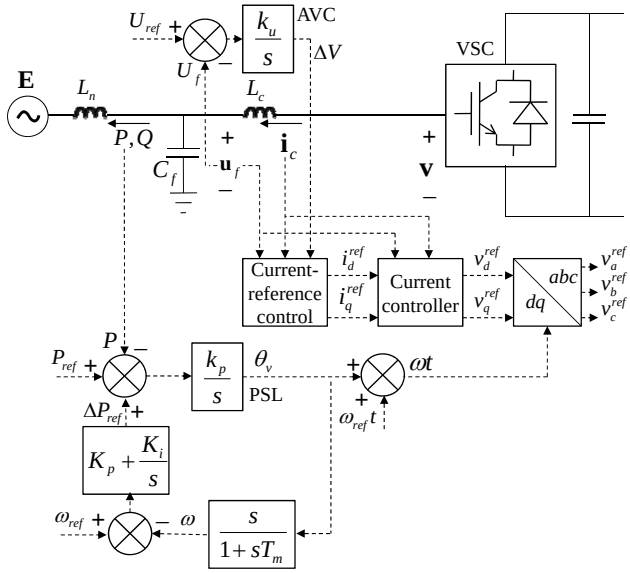

Figure 3: Power-synchronization control for HVDC converter station connecting offshore wind farm

$$\Delta V = \frac{k_u}{s}(U_{ref} - U_f) \qquad (2)$$

Up to this point, the control is very similar to power-angle control. However, in order to provide damping towards almost all possible resonance frequencies, the voltage-vector control law is formulated as follows:

$$\mathbf{v}_{ref}^c = (V_0 + \Delta V) - H_{HP}(s)\mathbf{i}_c^c \qquad (3)$$

Here (V_0) is the nominal voltage and $H_{HP}(s)$ is a high-pass filter for damping purpose and is expressed by

$$H_{HP}(s) = \frac{k_v s}{s + \alpha_v} \qquad (4)$$

This is the original scheme of power-synchronization control. Now, in order to have a current limiting capability as vector-current control, an additional control block, named current-reference control (Fig. 1) is included. The current reference is defined as

$$\mathbf{i}_{ref} = \frac{1}{\alpha_c L_c}[(V_0 + \Delta V) - H_{HP}(s)\mathbf{i}_c^c - H_{LP}(s)\mathbf{u}_f^c - j\omega_1 L_c \mathbf{i}_c^c] + \mathbf{i}_c^c \qquad (5)$$

Once the current reference is generated, the inner current controller behaves exactly the same way as vector-current control with a control law given by

$$\mathbf{v}_{ref}^c = \alpha_c L_c(\mathbf{i}_{ref} - \mathbf{i}_c^c) + j\omega_1 L_c \mathbf{i}_c^c + H_{LP}(s)\mathbf{u}_f^c \qquad (6)$$

The interesting feature of power-synchronization control is when the current is within the limit, the voltage reference is directly generated by (3). However, when the current hits its limits, the current control laws given by (5) and (6) come into picture. This can be easily verified by substituting (5) into (6).

While applying power-synchronization control for wind farm integration, the additional task is to maintain the frequency of the collection bus. In order to achieve that, frequency is extracted from the output of the PSL as shown in Fig. 3. The extracted frequency is then compared with the reference frequency of the collection bus and passed through a PI controller. Output of the PI controller is then added to the power reference of the active power controller. If the wind farm converter also takes part in controlling frequency, a droop character must be added to the frequency controller instead of the PI controller.

In addition to the power-synchronization control, the wind farm connecting HVDC station also has a chopper control function to dissipate the excess wind energy coming through the converter during fault in the onshore stations, into the chopper resistor present at station 1. The chopper control is a hysteresis type control, which is activated when the DC voltage goes beyond a certain value due to incoming energy from the wind farm side.

3.3 Control of the wind farm converters

The DFIG based wind farm uses back-to-back PWM converters for variable speed wind power generation. The grid side converter keeps the dc link voltage constant irrespective of the magnitude and direction of the rotor power. A stator flux oriented vector control is employed where the dc link voltage is controlled by the *d*-axis current and the reactive power at the point of common coupling is controlled by the *q*-axis current. The control strategy is well-established and can be found in [8]. The rotor side converter controls the active and reactive power from the stator. In order to achieve this, *d*-axis of the rotor reference frame is aligned with the stator flux vector. The *q*-axis current reference is generated from the commanded electrical power and the *d*-axis current reference is generated based on the reactive power requirement from the stator. The commanded electrical power is generated by the maximum power point tracking strategy discussed in [8], when the wind speed is below a certain value. The pitch control is not activated up to that point and the maximum possible energy corresponding to that wind speed is captured by the wind turbine. However, when the wind speed goes beyond a certain value, the power generated by the wind turbine is limited by the pitch controller. The relevant mathematical equations for the rotor side and grid side converter control are mostly similar to [8] and hence not described in this paper. The schematic diagram of the control strategy is presented in Fig. 4. All the symbols used in Fig. 4 carry their usual meanings and are explained in [9]. The compensation terms for the rotor side converter in Fig. 4 (v_{dr2} and v_{qr2}) are expressed as follows:

$$v_{dr2} = -s\omega_s \sigma L_r i_{qr} \qquad (7)$$

$$v_{qr2} = s\omega_s(\sigma L_r i_{dr} + L_m^2 i_{ms} / L_s) \qquad (8)$$

Where,

$$\sigma = 1 - L_m^2 / L_s L_r \qquad (9)$$

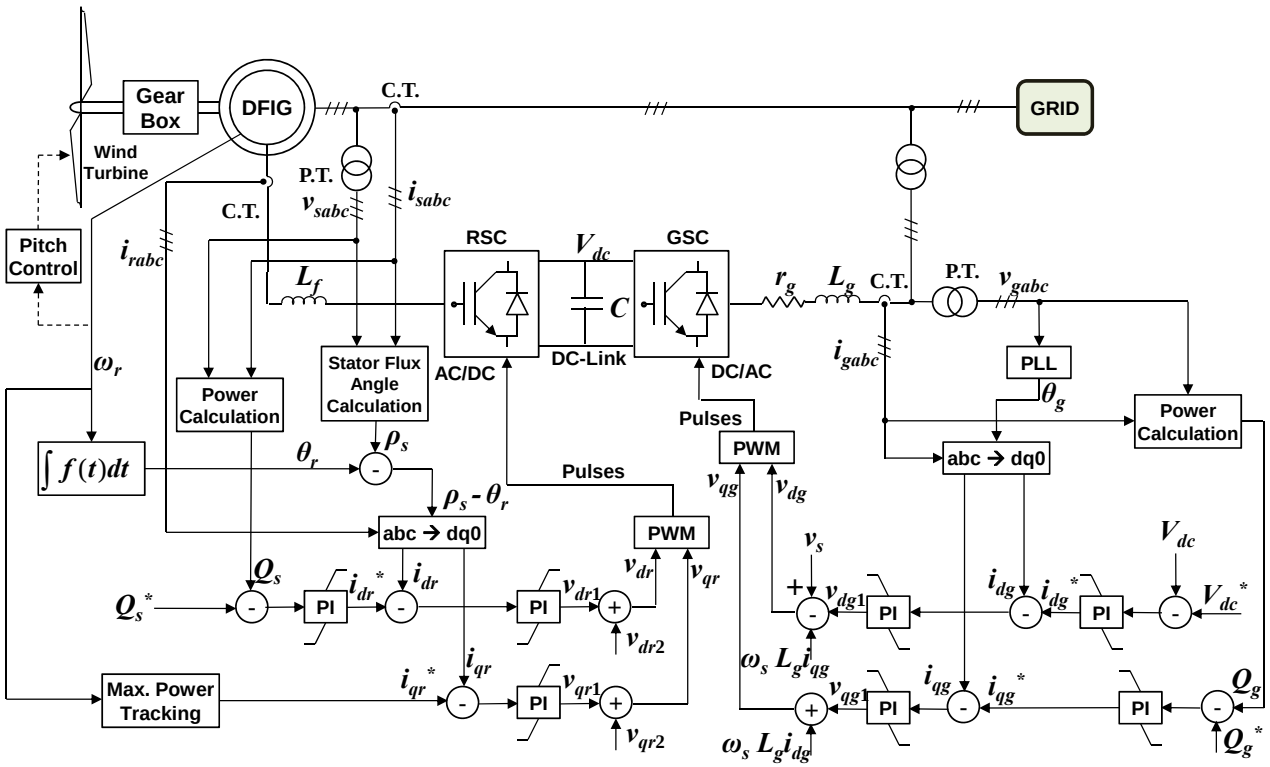

Figure 4: Control of the wind farm converters

4 Results

For the test system presented in this paper, it is assumed that the wind farm can generate 400 MW (0.67 p.u.) of power at a wind speed of 12 m/s. Station 1, which is the wind farm interconnecting station, transmitting the entire power generated by the wind farm to the DC side of the converter and thus behaving like a rectifier station. Station 3, the power controlling station, is also assumed to be acting as a rectifier and transmitting 180 MW (0.3 p.u.) of power from the AC side to the DC side. Therefore, Station 2, which is in DC voltage control mode, is acting as an inverter and transmitting the total power (close to one p.u) coming from the DC side of the other two rectifier stations to its AC side. In order to demonstrate the performance of the controller, three case studies have been presented at the operating point mentioned above.

4.1 Case study 1: Performance with wind speed variation

Initially the wind speed is kept at 10 m/s and at that wind speed the wind farm is generating approximately --- p.u. of power. Now, suddenly the wind speed is changed to 12 m/s. From Fig. 5 it is clearly observed that the additional amount of power generated by the wind farm due to the increase in wind speed is entirely passed through the DC voltage controlling station (Station 2). There is absolutely no change in the power flow through Station 3 and also in the DC voltages at Stations 2 and 3. However, there is a small change in the DC voltage of Station 1 in order to compensate for the additional voltage drop in the DC cable in between Stations 1 and 2.

4.2 Case study 2: Three-phase fault at Station 3

Now, a 100 ms three-phase to ground fault is created at the PCC of Station 3. During the fault, there is no power flow from the AC side to the DC side of Station 3. Therefore, there is a momentary drop in the DC voltage due to the discharging of the DC capacitor as shown in Fig. 6. However, the fast acting DC voltage controller of Station 2 reduces the power flow through it almost instantaneously and thus does not allow the DC voltage to go further down. Due to the quick action, Station 1 does not experience any disturbance at all during the fault. It is also observed in Fig. 6 that as soon as the fault is recovered, the power flows through Stations 2 and 3 come back to the pre-fault values without any significant overshoot. The smooth fault-ride-through actually establishes the correctness of the controller implementation.

4.3 Case study 3: Three-phase fault at Station 2

Maintaining the same operating conditions, similar fault is now applied at the PCC of Station 2. The fault does not allow the power to be transmitted from the DC side to the AC side of Station 2. Therefore, due to the incoming energy from the other two rectifier stations, the DC voltage starts increasing. As soon as the DC voltage goes to an abnormal value, the chopper control function of Station 1 allows the entire wind power to be dissipated in the chopper resistor. Due to the chopper action, the wind farm remains immune from the fault as shown in Fig. 7. It is also worth mentioning that the

auxiliary DC voltage control function of Station 3 plays its role during the fault at the DC voltage controlling station and thus reduces the power coming from the AC side to DC side of Station 3 during the fault.

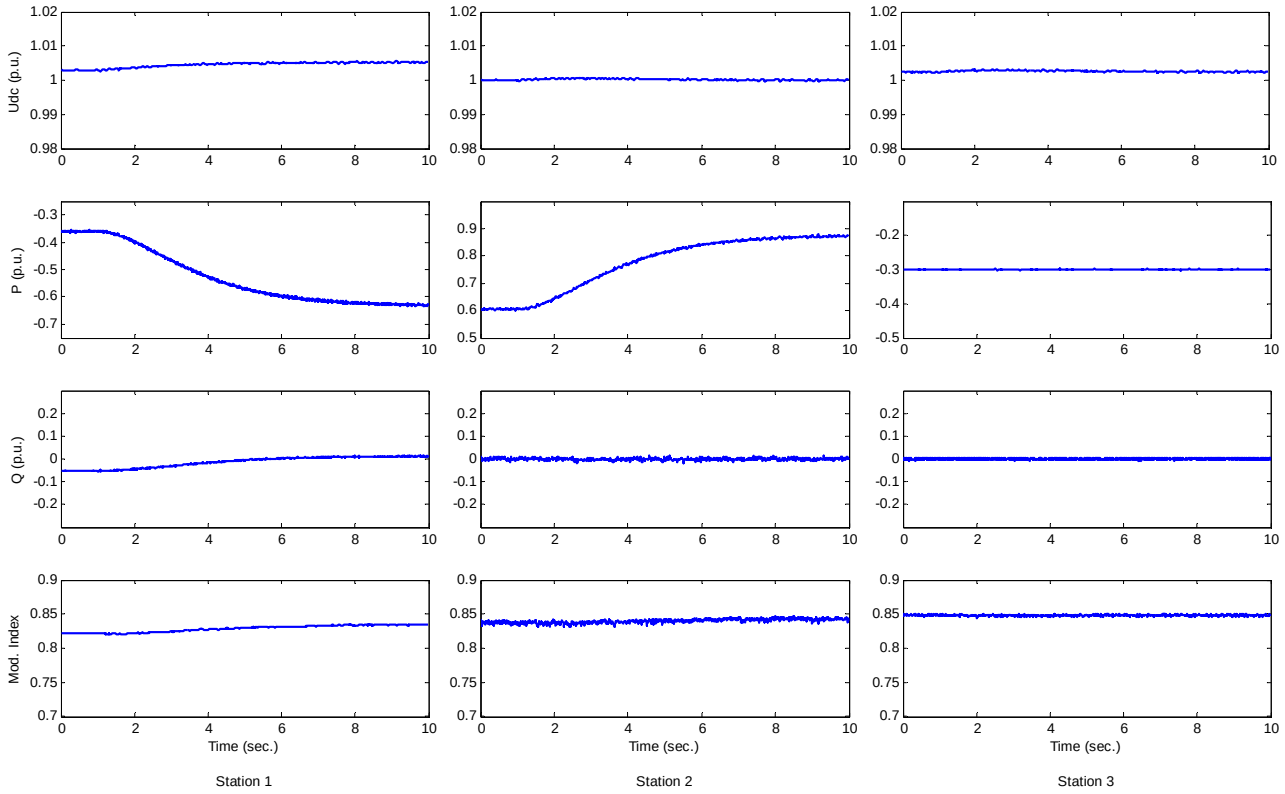

Figure 5: RSCAD results for wind speed variation

5 Conclusions

The real-time simulation studies of an offshore wind integrated multi-terminal HVDC grid have been presented in this paper. The model developed and presented here is based on RTDS internal control and will act as a building block for the future research in DC grid. The HVDC converter station which interconnects the wind farm employs power-synchronization control, whereas the other stations are based on vector-current control. Simulation results under wind speed variations and with different fault scenarios are presented. The satisfactory performance of the system during those situations demonstrates the efficacy of the control functions developed in RTDS.

References

[1] G. Asplund, B. Jacobson, B. Berggren and K. Linden, "Continental overlay HVDC-Grid," *CIGRE 2010*, pp. 1-9.

[2] M. Callavik, "HVDC Grids for offshore and onshore transmission," *EWEA Offshore Wind Conference*, 2011, pp. 1-5.

[3] E. Koldby and M. Hyttinen, "Challenges on the road to an offshore HVDC grid," *Nordic Wind Power Conference*, 2009, pp. 1-8.

[4] L. Zhang, L. Harnefors, and H.-P. Nee, "Power-synchronization control of grid-connected voltage-source converters," *IEEE Trans. Power Syst.*, vol. 25, no. 2, pp. 809–820, May 2010.

[5] L. Harnefors, M. Bongiornos, and S. Lundberg, "Input-admittance calculation and shaping for controlled voltage-source converters," *IEEE Trans. Ind. Electron.*, vol. 54, no. 6, pp. 3323–3334, Dec. 2007.

[6] L. Zhang, L. Harnefors, and H.-P. Nee, "Modeling and control of VSC-HVDC links connected to island systems," *IEEE Trans. Power Syst.*, vol. 26, no. 2, pp. 783–793, May 2011.

[7] L. Zhang, L. Harnefors, and H.-P. Nee, "Interconnection of two very weak AC systems by VSC-HVDC links using power-synchronization control," *IEEE Trans. Power Syst.*, vol. 26, no. 1, pp. 344–355, February 2011.

[8] R. Pena, J. C. Clare and G. M. Asher, "Doubly fed induction generator using back-to-back PWM converters and its application to variable-speed wind-energy generation", *IET Proc. Electr. Power Appl.*, Vol. 143, no. 3, pp. 231-241, May 1996.

[9] W. Qiao, R. G. Harley and G. K. Venayagamoorthy, "Coordinated reactive power control of a large wind farm and a STATCOM using heuristic dynamic programming", *IEEE Trans. Energy Conversion*, vol. 24, issue 2, pp. 493-503, 2009.

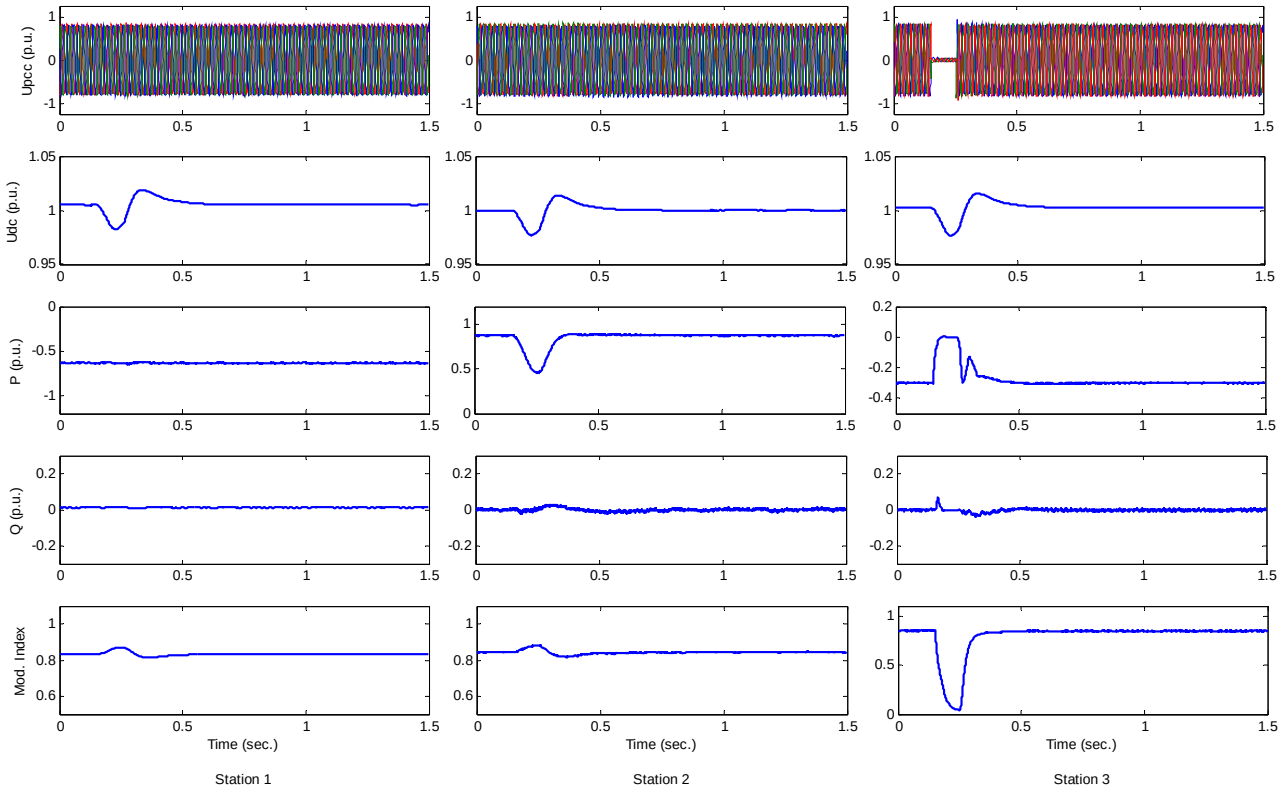

Figure 6: RSCAD results for a 100 ms three-phase fault at station 3

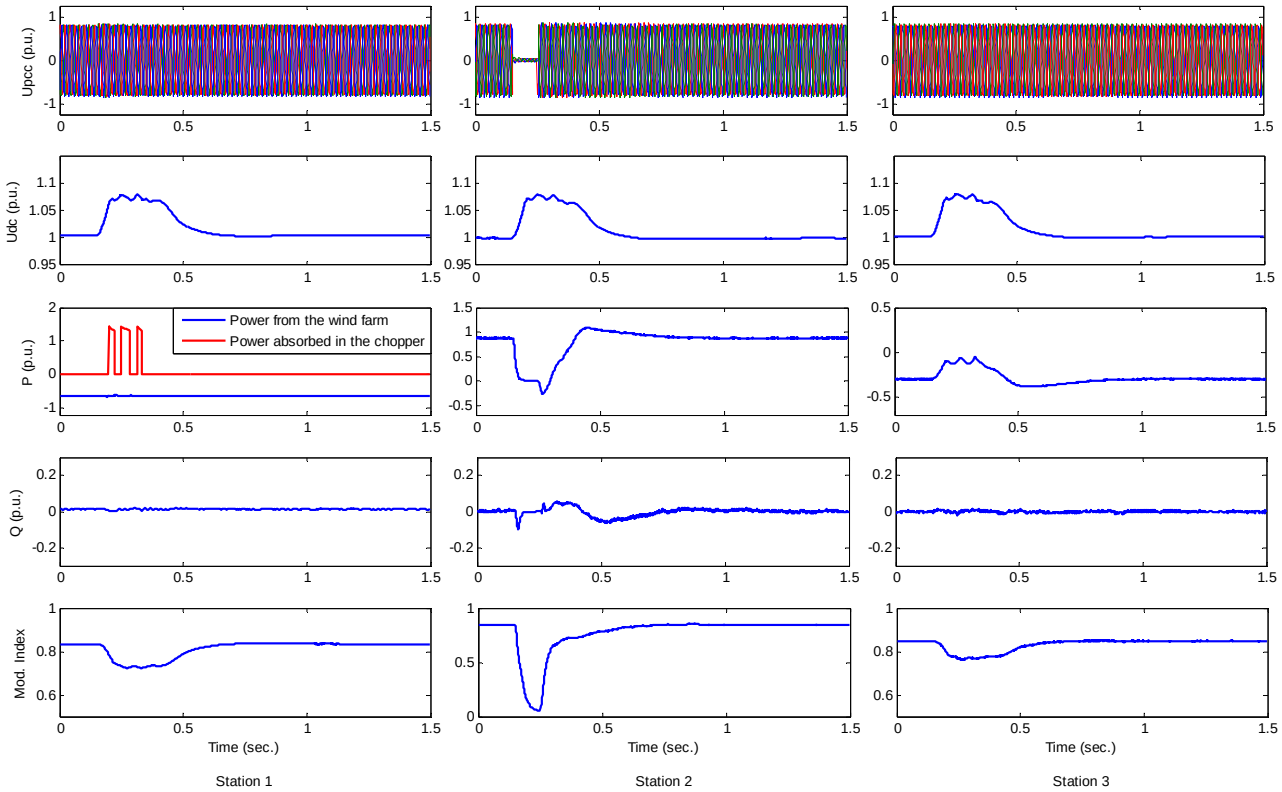

Figure 7: RSCAD results for a 100 ms three-phase fault at station 2